Probabilistic Low Cycle Fatigue criterion for nodular cast-irons

Fabien Szmytka, Eric Charkaluk, Andrei Constantinescu, Pierre Osmond

Probabilistic Low Cycle Fatigue criterion for nodular cast-irons

F. Szmytka[1a], E. Charkaluk[b], A. Constantinescu[b], P. Osmond[c]

[a]*IMSIA, CNRS, EDF, CEA, ENSTA Paris, Institut Polytechnique de Paris, 828 Boulevard des Maréchaux 91762 Palaiseau - France*
[b]*LMS - UMR CNRS 7649, Laboratoire de Mécanique des Solides, Ecole Polytechnique, Institut Polytechnique de Paris, Route de Saclay, 91120 - Palaiseau - France*
[c]*Groupe PSA, 212 Boulevard Pelletier, 78955 Carrières-sous-Poissy -France*

Abstract

This paper proposes an original method for characterising the Low Cycle Fatigue (LCF) lifetime using probability density functions. The protocol is based on statistics of microstructure heterogeneities taken as damage initiation sites, a qualitative mechanical analysis of the heterogeneities harmfulness and the definition of a micro-crack growth law. The technique is here established and the associated model identified for a nodular cast iron where the graphite nodules are assumed to be the damage initiation zones. The LCF lifetime is characterised from both a large set of experimental test between 300 and 600 °C and damage observations at the micro-scale. Experimental post-mortem observation combined with a simple numerical study first enable to assume the harmfulness of nodules according to their size and their probable role in the damage process A probability density function for the lifetime is then built from the following steps: (i) a quantitative analysis of the material micro-structure, which provides the probability density of nodules occurrence depending of their size (ii) an extreme value analysis using a Gumbel distribution and (iii) a micro-crack growth law associated with LCF conventional terms of energy densities. Its parameters are obtained using an optimisation process applied to laboratory fatigue experiment. The obtained probability function provides a good match for the lifetime and greatly improves results given by conventional criteria. It moreover provides a robust estimate of the lifetime scatter for different types of fatigue tests.

Keywords: High Temperature Low Cycle Fatigue, Thermomechanical fatigue,

[1]Corresponding author: `fabien.szmytka@ensta-paristech.fr`, email adresses of the other authors: `eric.charkaluk@lms.polytechnique.fr`,`andrei.constantinescu@lms.polytechnique.fr`, `pierre.osmond1@mpsa.com`

Cast-iron, Criterion, Microstructure, Probability of failure

1. Introduction

Cast-iron has been a traditional engineering material in the past centuries. Nevertheless, its castability, low price and mechanical resistance induces that it is still an actual materials of choice for parts exposed to high temperatures such as automotive exhaust manifolds or turbochargers. Nodular and compacted cast-irons are indeed still a strong material option despite recent technology innovations, such as cylinder heads with integrated exhaust manifolds [1]. Such structures operate at high temperatures where the material behaviour becomes strongly non-linear and exhibits viscoplastic effects. Moreover, exposed to large thermal gradients as well as severe mechnaical boundary conditions, they often experience high temperature LCF or even thermo-mechanical fatigue (TMF), that lead to the appearance of cracks during operation [2, 3, 4].

The state-of-art in design for these structures evolved in the last decades from prototype testing to virtual design performed using mechanical analysis software as proposed in a pioneering paper [5] for an automotive application. In order to keep the computational costs under control, they proposed as a main assumption to decouple material non-linear behaviour and damage provided the constitute model to be precisely identified. The structure lifetime is then associated with the initiation of a so-called macroscopic crack (of the order of a millimetre). The fatigue criterion then defines a number of cycles which is related to a local dissipated energy density as proposed initially by [6, 7].

The method has since successfully been applied on various structures by several authors, see for example [8, 9, 10, 11, 12, 13]. The fatigue criterion parameters are usually identified from conventional LCF tests [14] at different temperatures. The initial criterion has also been adapted to account for various effects, like mean stress or multi-axial loading [15, 16, 17]. The dissipated energy LCF criterion has thus been found to be rather robust[18]. Moreover, under LCF conditions, several groups [19, 20, 14] demonstrated that the criterion can be physically justified when damage and lifetime are mainly controlled mainly the propagation of micro-cracks at the micro-structure scale.

A major drawback of this method, however, is that it does not allow the estimation of fatigue behaviour randomness. Material fatigue failure has indeed a random aspect that can be observed through the scatter of the lifetimes for a given

load and the occurrence of various crack initiation zones observed during testing. The randomness of material properties, defects or even manufacturing variation cause the uncertainty of damage variable-lifetime relationship and seriously affect the dispersion of fatigue life. The previously discussed criterion has a deterministic formalism that thus prevent a reliable analysis of lifetime scatter, although it is highlighted in various studies especially when LCF is investigated over different temperatures [21, 22, 23, 24]. Moreover, recent probabilistic TMF design protocols for automotive parts relying on stress-strength interference analysis absolutely need a reliable estimation of this scatter [25]. Randomness is however usually introduced in the design process by a conservative strategy which induces most often arbitrary safety factors.

The aim of this paper is to overcome this fundamental drawback by enriching the criterion with a micro-mechanical analysis covering the random character of the damage initiation sites and keeping the computational complexity and costs of the design method at the same level as before. Several attempts have already been proposed in the literature in this direction. For example, Doudard and Calloch [26] included a Weibull distribution for the defects occurrence in order to explain the evolution of self-heating measurements for high-cycle fatigue (HCF). In the LCF domain, Maurel et al. [27] proposed a refined engineering fatigue model based on the dissipated energy and micro-crack growth law based on microstructural characteristics for stainless steels. A further step was proposed in Tabibian et al.[23] where pores in a lost-foam cast aluminium alloy are considered a initiation site for LCF micro-crack propagation. A statistical analysis of pores sizes is then combined with a micro-crack basic growth law and a standard LCF criterion in order to successfully predict the experimental scatter.

These previous attempts are then used as a basis to build a LCF fatigue criterion which explicitly incorporates the statistics of micro-structural defects responsible for the damage initiation. The material under scrutiny is a cast-iron for which a fatigue criterion is sought over a wide temperature range (300 to 600 °C). Such foundry alloys usual incorporate a large range of micro-structural heterogeneities which can evolve into damage initiation sites. In the particular case of cast-irons, carbides and graphite may appear in lamellar, compacted or spheroidal form and coexist with the iron matrix. Casting of complex parts also generate differential shrinkage and conduct to the formation of cavities or pores as documented in [28, 29]. The different phases and/or pores are randomly distributed in the material and often exhibit complex mythologies characterised by statistical distributions of size and shape. The study of their role in fatigue damage is commonly highlighted for high cycle fatigue[30] especially for aluminium alloys in [31, 32, 33, 34] and

for cast-iron in [35, 36, 37, 38, 39, 40].

In nodular cast-iron, "Void ratcheting" based on extended plasticity was identified as a potential mechanism leading to failure during experimental observations [41] and numerical investigations [42]. In a theoretical problem setting, Mbiakop et al. [43] showed, using finite element computations, that cyclic loading of pores steer the local plastic field and the pores evolution shape indicating the onset of cracks. Moreover, the study highlighted the importance of the local stress triaxiality and that kinematic hardening decreases the rate of the evolution when compared with isotropic hardening.In the other hand, the appearance of pores at the poles of graphite nodules has been observed in the literature [44] and it seems a reasonable assumption to consider them as potential initiation zones for fatigue micro-cracks. As a consequence, it is therefore relevant to evaluate their role in the case of high temperature Low-Cycle Fatigue. Let us further mention that under these loading regimes, the material exhibits generalised viscoplasticity and that strong differences in material properties between the nodules and the matrix naturally induce local strains and stresses concentrations, which may be accelerating factors in the damage process.

This article starts with a the presentation of the considered nodular cast-iron and the associated LCF tests and post-mortem damage analysis, which allows the hypothesis of considering graphite nodules as initial defects. A quantitative analysis of the micro-structure is then performed and the morphology of graphite nodules is examined by optical microscopy and digital post-processing. The observed data, size and shape characteristics, is then represented using probability distributions. Hypotheses are then formulated regarding the evolution of fatigue damage in the material. They are supported by the post-mortem tests analysis and by a qualitative numerical model that allow them to be refined and to finally propose, using the statistical theory of extreme values, the distribution of the largest nodules inside a representative elementary volume. Under cyclic loading, nodules are indeed considered as the origin of damage that propagates through micro-cracks until failure. A fatigue model is then proposed: it is based on this distribution and includes both micro-initiation and micro-propagation. As such, the path will complete the idea proposed in [5], with the missing micro-structural information and modelling while integrating ideas previously proposed bye Seifert et al. [45]. As a consequence it offers both the standard deterministic estimate of lifetime and an estimate of lifetime scatter. The parameters of the model are identified from a series of LCF experiments using a complete optimisation process. The final discussion exhibits their physical signification and examines the accuracy of the model to describe lifetimes of structures under thermo-mechanical loading by applying the

model on an experimental database outside the identification sample.

2. Experimental Database

2.1. Material and LCF tests

SiMo nodular cast-iron is widely used by the automotive industry, especially for exhaust systems as silicon and molybdenum enhance high temperature performances. The specific material used for this study present a ferritic structure up to 850 $°C$. Its chemical composition is given in Table 1.

C	Si	Mo	Mn	S	P	Ni	Cr	Cu
3.2	3.92	0.58	0.13	0.01	0.01	0.062	0.03	0.016

Table 1: Chemical composition of SiMo cast-iron (% in weight)

A quick analysis of the alloy micro-structure reveals the presence of a ferritico-pearlitic matrix but with a ferrite content between 85 to 90% depending on the observed areas. As seen on Figure 1, The micro-structure is also characterised by the presence of graphite nodules with a volume fraction of about 9%.

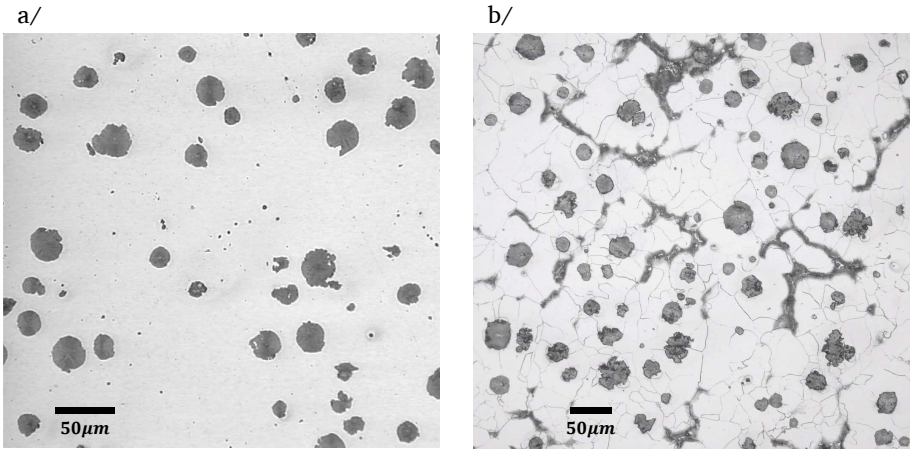

Figure 1: Microstructure of SiMo cast-iron without (a/) and with (b/) chemical etching

The study first focuses here on the Low Cycle Fatigue (LCF) of this cast-iron between 300 and 600$°C$. These temperatures present indeed a good compromise

in terms of material behaviour with an equivalent influence of classical plasticity (mainly kinematic hardening) and viscosity as shown by Szmytka et al. [46]. With conventional LCF lifetimes [5], the damage produced by the cyclic viscoplasticity can then be analysed without risks of high interference with oxidation or effects induced by the temperature history, typical in the case of TMF [47].

A complete experimental database is carried out for this alloy on cylindrical specimens with micro-structures representative of industrial parts (exhaust manifolds and turbochargers). This database is constituted of the tests performed by Constantinescu et al[5] at 350 and 600°C and completed with new tests at 300 and 500°C. For the latter, 120s-long hold times in tension or compression have been added in order to evaluate the influence of the mean stress on the lifetime. The total strain rate was $10^{-3}s^{-1}$ and the proportion between extreme strains was $\varepsilon_{max}/\varepsilon_{min} = -1$. Different strain amplitude $\Delta\varepsilon = \varepsilon_{max} - \varepsilon_{min}$ were tested and the experiments are summarised on Table 2. These tests constitute the identification database for the proposed criterion.

Temperature (°C)	Number of tests	Dwell phase	$\Delta\varepsilon$(%)	Lifetime
300	3	none	0.6-0.8	280-1100
300	2	tension	0.6-0.8	1050-1090
300	3	compression	0.6-0.8	260-1650
350	6	none	0.7-2.0	12-610
500	3	none	0.5-0.8	490-2620
500	5	tension	0.5-0.8	490-3700
500	2	compression	0.6-0.8	410-720
600	9	none	0.5-2.0	70-8190

Table 2: Low Cycle Fatigue tests condition summary

Observed lifetimes range between 100 and 8190 cycles and are therefore characteristic of LCF conditions. A single test has a very short lifetime that could be considered as outside the LCF range with 12 cycles. However, it was decided to keep this extreme point in the database, as the loading is still representative of the structures to be designed and provides useful information on the dispersion of the fatigue response.

2.2. Fracture surface analysis and damage mechanisms

Some specimens from the experimental basis were analysed to post-mortem quantify the influence of the micro-structure on the lifetime and on fatigue damage

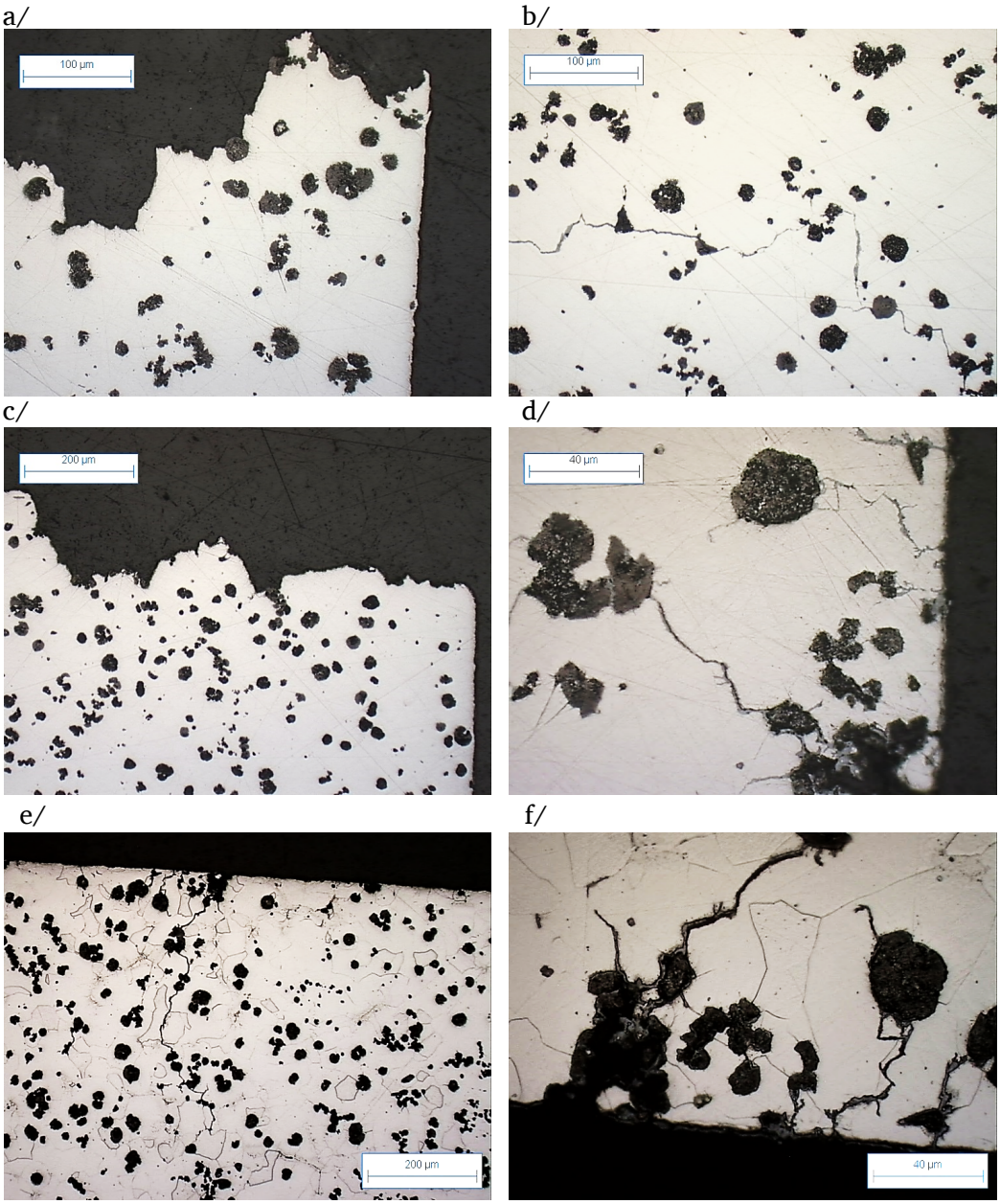

Figure 2: Fractography of LCF tested specimen at 300°*C* (a/ and b/) and at 500°*C* without (c/ and d/) and with (e/ and f/) chemical etching

mechanisms for this alloy. At 300°C, fatigue propagation area is fairly limited on the specimen, the crack propagation is indeed brittle for 95% of the gauge section. As shown in Figure 2.a and .b, the propagation occurs in the matrix while the crack path seems highly oriented by graphite nodules distribution. At 500 °C, fatigue propagation area is in the contrary fairly large (about 75% of the gauge section) but the same conclusions could be drawn. Fracture surface are indeed poorly oxidised and many secondary cracks are observed around the main crack, which justifies neglecting oxidation interference with damage mechanisms.

The observations reveal the important role played by the graphite nodules in the crack micro-propagation inside the ferritic matrix. Moreover, crack paths are enhanced and concentrated around the larger modules, as reported by several analyses in the literature [48, 41], The application of chemical etching on the observed surfaces unveil a trans-granular crack propagation. Additionally, let us remark that no pores or other casting defects have been observed on the studied surfaces. One can therefore assume that the fatigue crack initiation occurs in the vicinity of the graphite nodules and their size distribution is of prime importance in the micro-crack propagation, defining as such the main factors affecting the fatigue damage of this particular cast-iron.

2.3. Thermal Fatigue test : validation database

Thermal fatigue tests are also performed on a peculiar specimen by Constantinescu et al. [5] to validate their model. The experimental set-up described in their article is designed to induce very severe thermomechanical loads. In this experimental protocol, axial symmetric clamped specimens are heated by the Joule effect. The heating procedure produces a thermal gradient along the specimen axis, which also induces a variation of the mechanical fields in the same direction. This experimental set-up is presented on Figure 3.

The set-up, the imposed thermal loads and the adjustable rig stiffness that generates thermomechanical strains and stresses in the specimen are detailed in [5]. Eight identical tests were performed on the same nodular cast-iron between 40 and 700 °C with a heating rate of 20 °$C.s^{-1}$. The maximum temperature is obtained in a region of approximately 10mm in the centre of the specimen and with holding times between 30 and 900s at maximum temperature. The observed lifetimes are respectively 270, 503, 511, 551, 969, 1194, 1256 and 1388 cycles, underlying an important scatter in the fatigue behaviour. These tests will be our validation sample.

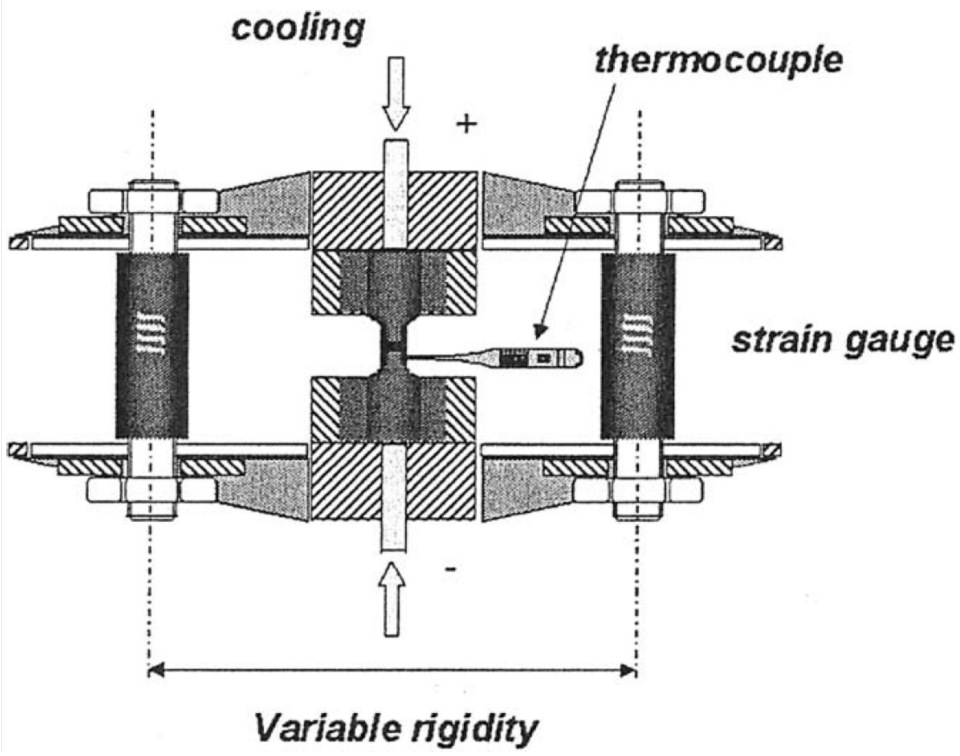

Figure 3: Thermal fatigue set-up from [5]

3. Quantitative analysis of micro-structure

3.1. Nodule population analysis and distribution modelling

Several samples from both fatigue specimens but also exhaust manifolds or turbochargers were analysed by optical microscopy. The obtained images were processed using Fiji software following a precise procedure for counting the number and measuring the size and shape of the graphite nodules, inspired by the work of [23] and [49]. 35 images of identical size were investigated for a studied surface of about $110mm^2$. The studied regions correspond to those which appear as critical regarding TMF (examples of exhaust structures and critical zones localisation could be found in [1]). All analyses were performed in two dimensions, for sake of simplicity for industrial parts and as it remains relevant in the global approach of a criterion based on micro-propagation.

Nodules Measure	$\tilde{\sigma}_1$	$\tilde{\sigma}_2$	$\tilde{\mu}_1$	$\tilde{\mu}_2$	Mean size - μm (for population 1)	Mean size - μm (for population 2)
Feret diameter	0.473	0.390	1.559	3.040	4.7	20.9
$\sqrt{area}$	0.444	0.402	1.229	2.757	3.4	15.8

Table 3: Statistical parameters for nodules size.

Statistical analysis of the size of graphite nodules was performed from the measurements in term of their Feret diameter and the square root of their surface, denoted next as a and $\sqrt{area}$ respectively. Figure 4.a and .b show the histograms of the nodules population distributed to the classes of the two types of measures. 14059 nodules were detected with Feret diameter, a, lying between 1.4 and 69 μm and the square root of their surface $\sqrt{area}$ varying between 0.83 and 53.8 μm.

For both dimensional measures, a and $\sqrt{area}$, one can recognise two populations of nodules: the first one consists in small nodules covering a majority of the total population while the second one is constituted of medium or large size nodules covering a minority of the total population. Similar observations have also been reported in [49] and accordingly we propose to represent the population by double log-normal distributions expressed as:

$$p_s = \frac{1}{s\sqrt{2\pi}\tilde{\sigma}_1\tilde{\sigma}_2}\left[\tilde{\sigma}_2 \exp\left(-\frac{1}{2}\left(\frac{ln(s)-\tilde{\mu}_1}{\tilde{\sigma}_1}\right)^2\right) + \tilde{\sigma}_1 \exp\left(-\frac{1}{2}\left(\frac{ln(s)-\tilde{\mu}_2}{\tilde{\sigma}_2}\right)^2\right)\right] \quad (1)$$

where s is the nodule size. $\tilde{\sigma}_{1,2}$ and $\tilde{\mu}_{1,2}$ denote the mean value and the standard deviation of each log-normal distribution. The optimal parameters identified from

the measured data are displayed in Table 3 and the comparison of the measured and estimated histograms are displayed in Figure 4.c and .d. One can further remark an excellent match between the measurement and the model.

The average sizes of the two populations of nodules are relatively close for both measures as the Feret diameters and the $\sqrt{area}$ with 20.9 and 4.7 μm and 15.8 and 3.4 μm respectively. There are small differences in the histograms, especially for the population of small nodules which are more numerous and less dispersed for their geometric size. Next, we will only consider the Feret diameter distribution for the construction of the fatigue criterion which seems perfectly suited to describe nodules size even if the square root of the surface $\sqrt{area}$ is a recognised measure of the default size of particles (in terms of results for the identification of fatigue criteria and for all the conclusions of following sections, this choice has anyway very little influence).

3.2. Shape of nodules

The particular shape of the nodules conducts to stresses and strains concentrations due to the contrast of mechanical and thermal expansion material parameters between the nodules and the ferritic matrix. Nodules can therefore act as onset of damage zone for the considered material. It is well known from classical elasticity theory that the concentration will be inverse proportional with the curvature of the shape. However it is straightforward that the exact 3D shape of the nodules cannot be recovered without tomography measurements that conducts to explosive costs when applied to large population on industrial parts. Therefore, a single scalar, the circularity c, is further assumed as the appropriate ans statistically representative parameter for representing the shapes of the population of nodules. Circularity c is defined for a particle with an area of A and a perimeter p as :

$$c = 4\pi \frac{A}{p^2} \tag{2}$$

It reaches 0 for infinitely elongated polygon and 1 for perfect circles. Figure 5.a displays the distribution of nodules according to their Feret diameter and their circularity. A quick analysis shows that the population of smallest nodules presents a circularity essentially close to 1. This is undoubtedly due to the resolution of the images used for the nodules statistical analysis: these very small elements can be assimilated to areas mainly concentrated in squares of 2 pixels on each side. The circularity of the small elements is therefore not necessarily relevant here. However, as will be specified in the following sections, it is essentially the larger nodules that are of interest in the formalism we develop for fatigue.On the other hand, the largest nodules have a lower circularity, between 0.75 and 0.9. Their

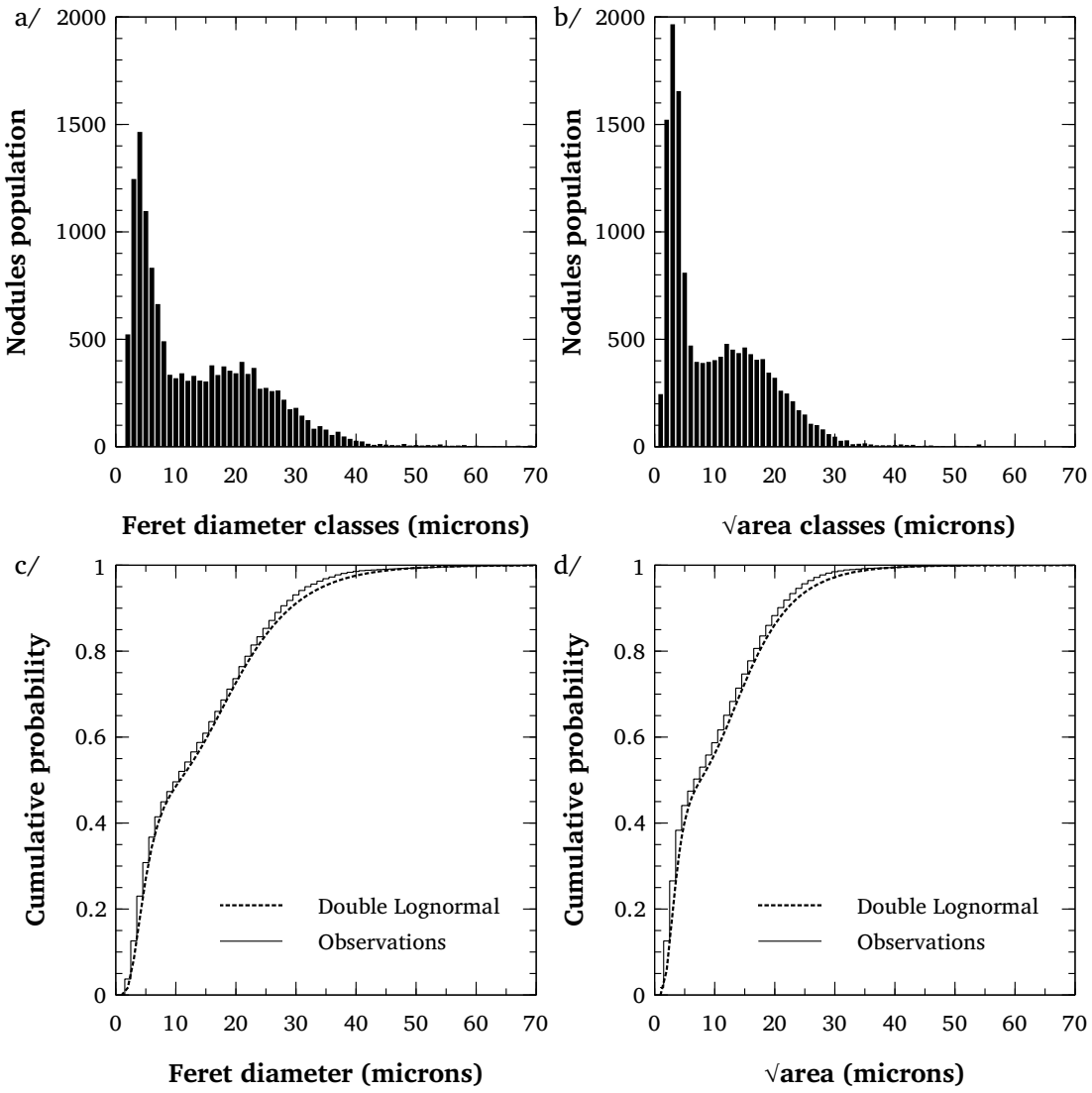

Figure 4: Histogram of nodules populations based on their Feret diameter (a/) and their $\sqrt{area}$ (b/). Nodule size probability estimated by a double Log-normal distribution for Feret diameter (c/) and $\sqrt{area}$ (b/)

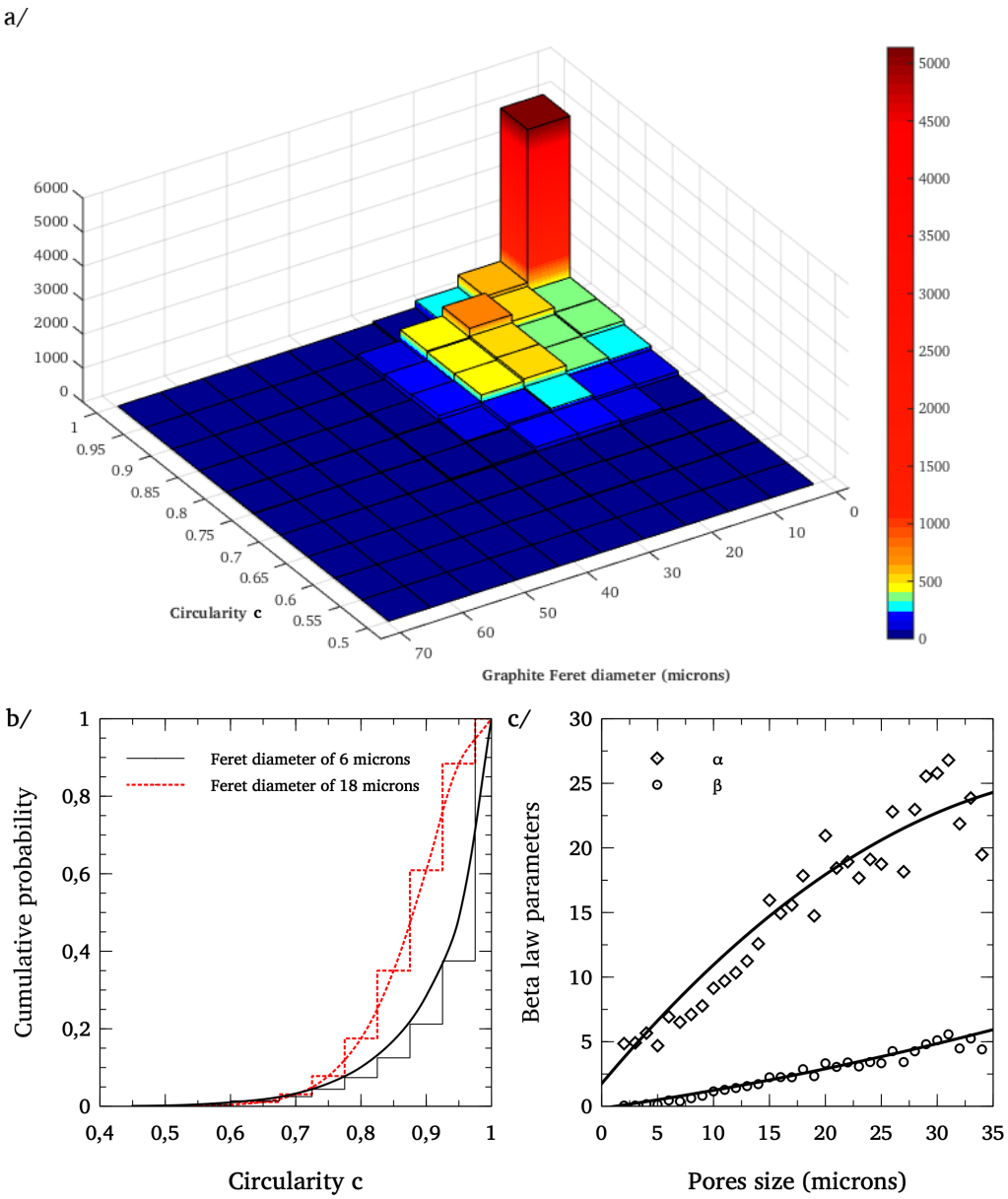

Figure 5: Graphite nodule : observed circularity distribution versus nodule size (a/) Beta distribution for different size (b/) and Beta law parameters (c/)

morphology, visualised here in 2D, presents a segmented border with punctually zones with an important curvature. This can be explained by their rapid growth during the alloy solidification and the loss of stability of the material interfaces. Moreover, the nodule population with a circularity smaller than 0.75 is extremely reduced. As a consequence, in each class of nodule size, the statistical distribution of the circularity of the nodules can easily be represented by a beta law, expressed as :

$$p_c = \frac{\Gamma(\alpha+\beta)}{\Gamma(\alpha)\Gamma(\beta)} c^{\alpha-1}(1-c)^{\beta-1} \tag{3}$$

with c, the circularity. α and β are the parameters of the distribution. The evolution of these two parameters with the nodule size in microns are presented on Figure 5.c. Their evolution can be represented by simple models, as for example the second-order polynomial estimation used here. A good match of the circularity distribution is displayed on Figure 5.b for 2 classes of nodule size.

With the size and circularity of nodules now fully available and formalised using statistical distributions, the role of nodules in the damage process and the integration of these distributions in a fatigue criterion can now be discussed.

4. From defects to lifetime

4.1. Damage initiation and evolution theory

From the engineering point of view, TMF or high-temperature LCF failure of a part, at the macro-scale, is usually related to the apparition of an observable crack, the length of which sufficient to break a material representative volume element (RVE). This failure is the resulting action of the evolution of irreversible processes that occur at the material micro-scale. For nodular cast-irons, macroscopic failure can be linked to the progressive damage of each of its constituent phases as underlined in [28, 52]. From a meso-scale point of view, damage can occur as spheroid rupture, ductile damage in the ferritic matrix or spheroid/matrix debonding. These micro-mechanisms of failure are controlled by the macroscopic load imposed to a RVE [53].

From an experimental point of view and in accordance with what was presented in the section detailing the material and the LCF tests, the important role of graphite nodules in the damage cannot indeed be put aside. Several studies in the literature in the context of low cycle fatigue at room temperature have highlighted this role and observed the classic damage mechanisms of cast iron in the

case where plasticity is generalised in the material. Thus, Harada et al.[54] then Komotori et al.[55] have pointed out, on various loading regimes, that cracks occurring for ferritic cast-irons result from the coalescence of micro-voids originated from debonding of the matrix/graphite interface. Later, Bubenko et al. [56] showed that the low-cycle fatigue cracks always start at the interface between the graphite nodule and surrounding ferrite matrix, while graphite nodules remain generally unbroken. Canzar et al.[57] proved that size, shape and distribution of the graphite nodules has no significant influence on cyclic hardening of the material but that they play a major role in the crack initiation and propagation process. They showed that the larger irregularly shaped nodules tend to reduce fatigue strength. All these observations therefore suggest that the damage mechanism corresponds essentially to the location of plastic stresses and strains around the largest nodules which, after decohesion of the matrix/nodule interface, act as pores where micro-cracks initiate.

From a numerical point of view, nodular cast irons have given rise in the literature to numerous studies on plasticity and damage at the microstructural level, and in particular on the behaviour of graphite nodules in a ductile ferritic matrix. Many authors have thus carried out simulations of representative elementary volumes in order to better understand the interactions between the matrix and the nodules and to develop damage models based on the nucleation, growth and coalescence of cavities in a solid fraction.[58, 59, 60, 61, 62, 63]. In the simulations, considering easy decohesion of graphite nodule and ductile matrix, the graphite nodule is modelled either as a void or as a rigid particle in the cell model [64]. The cyclic elastoplastic computation of a representative element volume with a spherical pore in its center discussed in [67] is thus an interesting starting point. Authors show that the dissipative mechanism are maximal at the interface of the matrix with the pore. Moreover the shape of the zone encompassing the maximal dissipation, which is at the origin of damage are located in most of the cases around the equator of the pore and provide an ideal initiation for the fatigue crack propagation. The fact that the results in [67] have similar shapes for isotropic or kinematic hardening indicates that the results obtained with the particularly chosen viscoplastic material behaviour can be generalised to other configurations.

Considering all these observation, a high-temperature LCF damage initiation and propagation process can be proposed. The mechanical behaviour of spheroidal graphite cast irons is indeed clearly influenced by their generally heterogeneous microstructure (composed at first order of a ductile ferritic matrix and fragile graphite spheroids). These latter naturally induce stress concentrations and quickly lead to debonding and pore generation. It then seems realistic to consider that they will be the sites of early LCF or TMF damage. The stress concentration is a function

of the size and the shape of the considered nodules ; the most significant damage shall thus appear first on the largest and least spherical particles. In the rest of this article, we will decide not to take into account either the influence of neighbouring nodules on the mechanical fields around a considered nodule, or the existence of possible aggregates of particles that could be the consequence of the solidification process and generate an increase in local mechanical fields. These two elements can legitimately play a role in the damage mechanisms and may be investigated later.

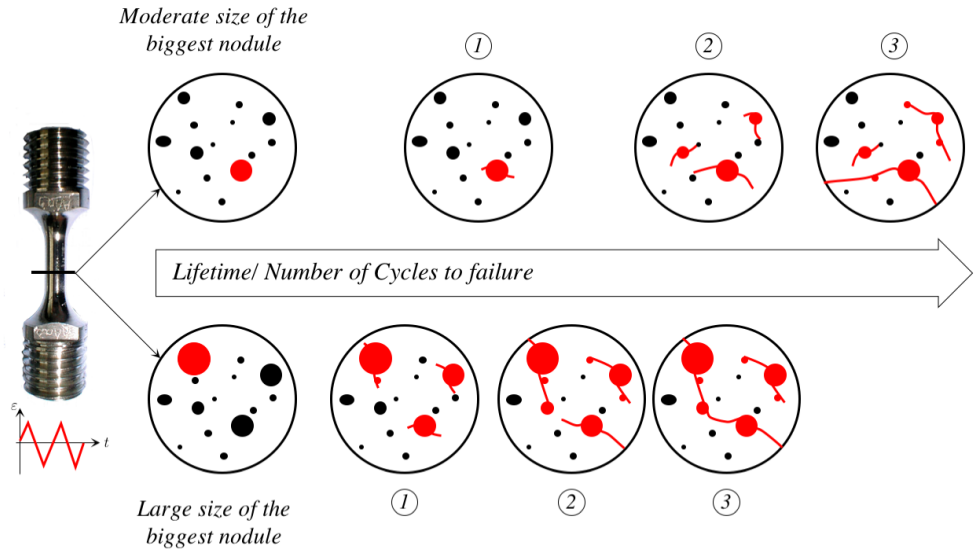

Figure 6: Simple hypothesis of damage evolution as a function of the maximum nodule size within a volume element loaded by an identical load

Based on the preceding results, we can make the simplifying assumption that within a representative elementary volume containing a large family of graphite nodules in cast-iron, the damage will then localise around the largest graphite nodule with the lowest circularity. The localised dissipation mechanisms will initiate a micro-crack which will propagate from this nodule as illustrated on Figure 6. The crack initiation will relax the local load and with increasing number of cycles further micro-cracks will appear on smaller nodules. With further cycles micro-cracks will start to propagate until coalescence inducing the complete failure of the

volume element under consideration. The failure of the volume element represent the initiation of a macroscopic crack and the onset of the structural failure.

We shall further infer that propagation is mainly driven by the material behaviour of the ferritic matrix. Comparable phenomena have been observed on aluminium alloys under similar loading conditions [66]. One can conclude that the lifetime of a representative volume element, i.e. number of cycle to the initiation of a macroscopic crack is dependent on its the largest graphite nodule and the properties of the matrix.

4.2. Extreme value statistics

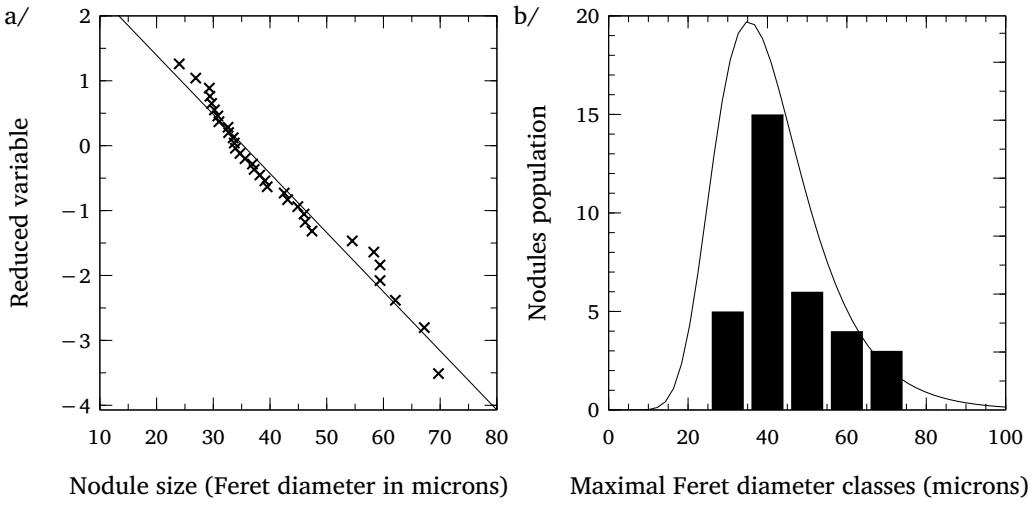

Figure 7: a/ Gumbel probability plot ; b/ Gumbel identified distribution for given classes of maximal nodule size for each sample

Once the damage mechanism are assumed, a discussion has to be conducted on the type of distribution to be used to represent graphite nodules in a fatigue context. Tabibian et al.[23] introduce a simple distribution of pore size into a micro-crack propagation law for an aluminium alloy. This choice is simple and can be improved as it is strongly related to the size of the zone used to identify the distribution without taking into account of distribution tail estimation..

For high-cycle fatigue, the statistical theory of extreme values is very often used to represent the distribution of the largest particles or defects observed on

a plane section of fixed area [30]. In our case, considering the total distribution of nodules would be possible but certainly too simplistic. Indeed, the over-representation of small nodules would undoubtedly favour the calculation of very long lifetime, which is far to be conservative. Here, the statistical measurements of nodules size and circularity have first been carried out on surfaces with a constant area chosen to be representative both of critical areas observed on the parts to be designed and to specimens failure area (size equivalent of circle with 1mm radius). A sample of observations of maximum sizes of nodules for each investigated optical microscopy picture can then be obtained and serve as a basis for an extreme values distribution. As explained by Beretta et al.[65], extreme value theory allows us to know the asymptotic behaviour of the maximum taken by the values of identically distributed and independent random variables. This law includes parameters that can be estimated on the basis of the extreme values taken in blocks of fixed size for the available data, which is the case here as detailed in section 3.1. Here, the extreme value distribution arises as the possible limit distributions for the maximum value of nodule size considering a given area. For the 35 pictures analysed, we obtained the following sample

Picture	Max. size (μm)	Picture	Max. size (μm)	Picture	Max. size (μm)
1	37.2	13	44.9	25	54.5
2	30.2	14	47.4	26	39.5
3	33.9	15	38.2	27	46.0
4	42.5	16	43.1	28	30.8
5	58.3	17	35.6	29	59.4
6	69.7	18	33.7	30	67.2
7	69.8	19	39.1	31	29.7
8	69.5	20	29.3	32	59.4
9	46.2	21	29.4	33	62.1
10	32.6	22	34.7	34	37.6
11	32.7	23	26.9	35	31.2
12	31	24	24.0		

Table 4: Maximal nodule size value per investigated image.

The Gumbel plot assess the fit of data sample to the Gumbel distribution. It implies first that the maximum values to be arranged in increasing order. It induces a so-called reduced variable which is equal to $\ln(\ln(i/n + 1))$ with n the sample size and i, the i^{th} smallest maximum value. This variable is plotted versus the corresponding value of nodule maximal size. A straight line indicates a good fit to

the distribution which is here the case as seen on Figure 7.a. A Gumbel distribution is then identified for the sample and plotted on Figure 7.b. The probability that the biggest nodules on a critical zone has a size equal to a is expressed as

$$G(a) = \exp\left(-\exp\left(-\frac{a-\lambda}{\delta}\right)\right) \tag{4}$$

with λ and δ, two parameters respectively identified to 35.28 and 10.97 . This distribution will then be taken as the probability of finding maximum nodules either in the fatigue specimens or in the part critical zone[65]. Here, circularity is not directly taken into account. It simply allows us to consider the largest nodules as the most critical. A finer integration by considering, for example, a combination of the largest nodules with the lowest circularity could be envisaged but it would require a heavy additional work of fine analysis of the role of the nodules morphology in the fatigue process.

4.3. A probabilistic fatigue criterion

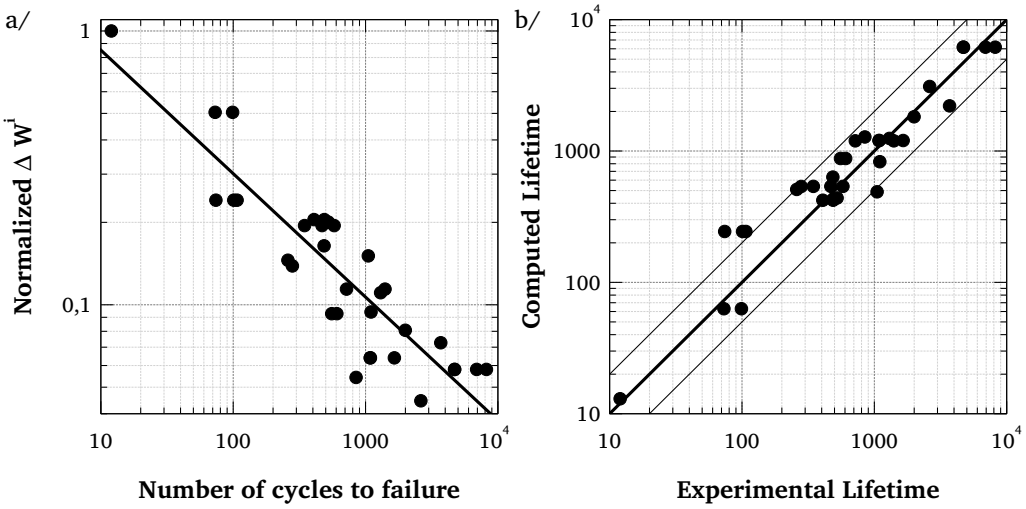

Figure 8: Deterministic fatigue criterion

The relation between viscoplastic dissipated energy over the stabilised cycle and the number of cycles to failure has proven to be a robust fatigue criterion starting with the first results by Skelton, the development including structural computational proposed in [5] and the evolution including mean stress in [16, 17]. If

the viscoplastic dissipated energy over the stabilised hysteresis loop is denoted W^p and the number of cycles to failure, N_f, the criterion takes the following form:

$$W^p N_f^b = \int_{cycle} \underline{\underline{\sigma}} : \underline{\underline{\dot{\varepsilon}}} dt N_f^b = c \tag{5}$$

where b and c denote two material parameters identified using a database of isothermal LCF tests. The direct application of this fatigue criterion, proposed by [5] over the present cast-iron LCF database appears to be fairly robust as it revealed by the results in Figure 8. However, the scatter of the data characterised by the coefficient of determination R^2 equal to 0.80, stay important and cannot be precisely determined. As a partial conclusion, one can state that the energy density remains a reliable marker for fatigue damage, but can neither accurately estimate the variability of the fatigue response nor explain the role of the microstructure.

As an outcome, we propose to combine the description of the microstructure variability proposed Charkaluk et al.[23] which will provide the mathematical form of the criterion with the micro-crack propagation law advanced in Maurel et al.[27] for ferritic stainless steels. As matter a fact, the failure probability p_f of an elementary volume element can be described using the probability of finding a graphite nodule of maximal size a_0 within this RVE according to the formula:

$$p_f = \int_{a_0}^{a_f} \frac{da}{\left(\frac{aW^p}{\gamma_p}\right)^{m_p} + \left(\frac{aW^e}{\gamma_e}\right)^{m_e}} \tag{6}$$

$$W^e = \frac{1}{3} \int_{cycle} tr\left(\underline{\underline{\sigma}}\right) tr\left(d\underline{\underline{\varepsilon}}^e\right) \tag{7}$$

with $\underline{\underline{\varepsilon}}^e$, the elastic part of the strain tensor and γ_p,γ_e,m_p,m_e are four parameters to be identified. a_0 is here a random variable representing the size of the largest nodule and taken as a initial defect size. a_f is the final length of micro-crack, propagated from the nodule. It is associated with a critical or unacceptable crack for the part or specimen under scrutiny. The size of a macroscopic crack on a laboratory fatigue test specimen that induces final failure is in mm size, while on a structure final failures are induced by cm or dm size crack. As already discussed in [23], it seems reasonable to choose a critical size a_f = 2mm.

The final form of the criterion is however relatively simple. This is a direct consequence of a series of underlying hypothesis as well as the absence of possible interaction of the different micro-cracks, i.e. the one starting at large nodules with the ones starting at smaller ones. In order to be conservative, a shorter value of $1mm$ is therefore used.

5. Results and discussion

5.1. Criterion identification

Let us first remark that the number of cycles to failure N_f are considered next as a random variable. Its probability distribution is directly linked with the previously identified Gumbel distribution for maximal nodule size. Starting from this observation, one can identify the criterion fatigue parameters from the LCF experimental lifetime results, by matching the probability distribution for the number of cycles to failure and failure probability expressed in equation 6. The probability for the number of cycles to failure is directly dependant of the loading condition on a part or more easily of the load applied on a specimen. These conditions are represented by the couple (W^p, W^e) that can easily be computed from the monitored strains and stresses evolution. Nf is here considered to follow a log-normal distribution for the sake of simplicity:

$$p_{f,(W^p,W^e)}(N) = \frac{1}{2\pi N \sigma_{(W^p,W^e)}} \exp\left(\frac{(\ln(N) - \mu_{(W^p,W^e)})^2}{2\sigma_{(W^p,W^e)}}\right) \tag{8}$$

The distribution parameters $\sigma_{(W^p,W^e)}$ and $\mu_{(W^p,W^e)}$ can be identified from the nodule size Gumbel distribution. A number of cycles to failure can indeed be computed for each class of nodule maximal size obtained from the Gumbel distribution (an example of classes is represented in Figure 7). For each class, the corresponding maximal value is introduced as a_0 in equation 6, introducing chosen values for γ_p,γ_e,m_p and m_e. This step leads, for a given loading condition (W^p, W^e) to a complete histogram for the number of cycles to failure and the log-normal parameters are then easily identified with the computation of the mean value and the standard deviation of the identified population.

It is then easy to compare the mode of this distribution (depending on the 4 parameters γ_p,γ_e,m_p and m_e of equation 6) with the actual result of the LCF test for which (W^p, W^e) were induced by the loading conditions on the specimen. A least-square cost function is then calculated and its minimisation allows us to obtain the optimal values for γ_p,γ_e,m_p and m_e. The results of this simple least-square optimisation are presented in Table 5.

Parameter	$\gamma_p(mJ.mm^{-2})$	$\gamma_e(mJ.mm^{-2})$	m_p	m_e
Optimized value	4.29	5.51	2.57	2.02

Table 5: Optimized criterion parameters

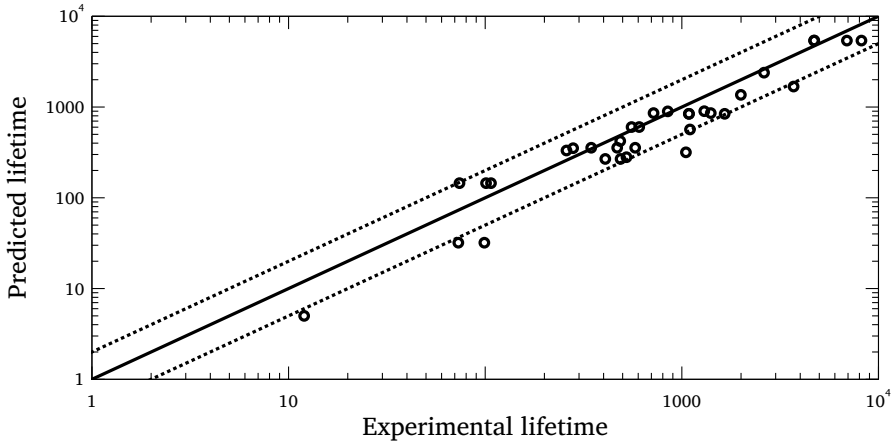

Figure 9: Experimental versus predicted lifetime with the proposed criterion

The comparison of these results with those obtained by Maurel et al.[27] on stainless steel only at 300°C is interesting. The LCF tests are indeed carried out under identical conditions and Maurel had chosen the grain size as the initial crack size for deterministic results. The parameter m_e has been set at 2 in the case of stainless steel, consistent with traditional databases, which is very close to the value we obtained through optimisation. This result, for two ferritic matrices, underlines the robustness of our identification process. Taking into account Maurel's formulation which introduces a correction related to grain size in mathematical formalism, we find very similar values also for γ_e. The contribution of the "elastic" part for two ferritic matrices therefore seems to be similar here. However, the viscoplastic part is much more pronounced in the context of the considered cast-iron: indeed, m_p is here higher (2.57 against 1.62), thus accentuating the viscoplastic contribution to propagation, which also sees its attenuating factor γ_p decrease by a factor of 10 (once again by taking into consideration the grain size correction from Maurel and his co-authors). These differences can be partly explained by the high viscoplasticity of the considered cast-iron for high temperatures, much higher than that of stainless steel considered by Maurel and his co-authors at 300°C as previously shown in a comparative study[47]. This high viscoplastic activity greatly reduces the observed stress levels and ultimately the W^p ones. To obtain a sufficient and significant driving force for the damage, the adjustment of the parameters of the propagation law appears logical. For a given pair (W^p, W^e), the distribution mode is furthermore given by:

$$N_{computed} = \exp\left(\mu_{(W^i,W^e)} - \sigma^2_{(W^i,W^e)}\right) \tag{9}$$

This value is compared to the experimental one on Figure 9 which underlines a very good matching between computed and experimental lifetime. The correlation coefficient R^2 is here equal to 0.92, reaching a higher value than the deterministic criterion detailed previously. The proposed method supplies therefore a lifetime estimation at least as effective as the deterministic criterion. However, additional information in the probability density functions of failure are an important improvement as it is possible to now estimate the scattering of the fatigue strength for the material.

5.2. Criterion validation

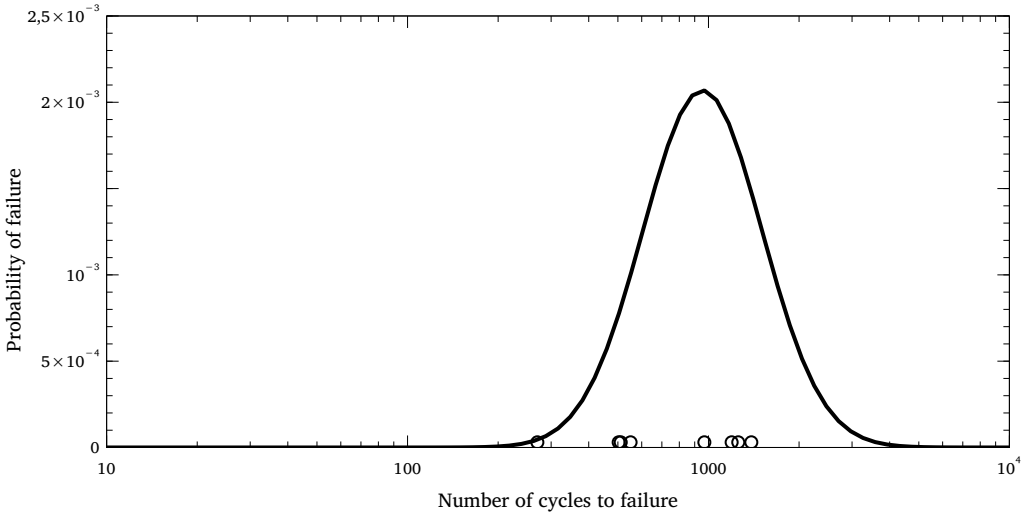

Figure 10: Probability of failure distribution for thermal-mechanical structural tests[5]. Circles represent experimental lifetimes.

The thermal fatigue tests presented in section 2.3 is here used as a validation sample for the proposed criterion. They are simulated in Abaqus using an elasto-viscoplastic behaviour detailed in [68]. The clamp value due to the variable stiffness (proportional to the flexural moment of the beams) is here fixed at 183 000 N/mm and the dwell time at 700 °C at 60s. The thermal load of this experiment was numerically estimated by an electric and a thermal FEM computation on Abaqus.

The results of the thermal-electrical computation is then introduced in a mechanical computation. The FE model is here constituted of 43934 nodes and 28805 C3D10 10-node quadratic tetrahedral elements. The numerical protocol that enables to detect the most critical finite element for thermomechanical fatigue are explained in [5]. For these tests, the obtained values of W^p and W^e for the most critical element are respectively 1.44 and $0.44 mJ.mm^{-3}$ and allow the identification of a number of cycles to failure distribution using the parameter set identified on the LCF database as shown on Figure 10 where the experimental lifetimes are figured by circles. The Figure represents the probability density for the number of cycles to failure and the considered load. An fair good representation of the variability of the fatigue response is highlighted with most of the tests lifetimes in the high probability zone and a very relevant estimate of the average lifetime (about 1150 cycles versus 850 experimentally). Thus, despite the limited temperature range for model identification, satisfactory initial results in thermomechanical fatigue can be obtained, which constitutes a first validation of the criterion.

6. Conclusions

This paper proposes a method for estimating the probability density distributions of lifetime in high temperatures LCF and by extension in TMF for nodular cast irons. It is based on the estimation of the probability density of nodule sizes using optical microscope image analysis and identifying a double log-normal distribution. After analysis of the fatigue test results supplemented by literature analyses, nodules are identified as the preferred initiation zone. A probability density function over the lifetime is then proposed based on an extreme value Gumbel distribution for nodule maximal size and a micro-crack propagation law integrating energy densities identified on the loading cycle. The four parameters of the proposed criteria are optimised to have the most probable estimated lifetimes that correspond to the experimental observations. The proposed criterion provides predictive results for the studied cast iron, while the lifetime probability is explicitly calculated and successfully estimates the results obtained with thermal fatigue tests. The parameters identified for the model are also consistent with the literature and physics of damage for such cast-iron.

The discussed model is based on a series of material assumptions, i.e. the type and shape of the nodule, which must be adapted each time the method is extended to a class of materials. The ability of such a model to correctly describe low cycle fatigue behaviour at higher temperatures (presence of oxidation, decarburisation) is not guaranteed and it goes without saying that it should be modified to be effective. The ability to predict lifetime in TMF should also be explored in more detail,

particularly for wider range of thermal load.

References

[1] F. Szmytka, P. Michaud, L. Rémy, A. Köster, Thermo-mechanical fatigue resistance characterization and materials ranking from heat-flux-controlled tests. Application to cast-irons for automotive exhaust part, International Journal of Fatigue, Volume 55, 2013, Pages 136-146,

[2] A. Benoit, M.H. Maitournam, L. Rémy, F. Oger, Cyclic behaviour of structures under thermomechanical loadings: Application to exhaust manifolds, International Journal of Fatigue, Volume 38, 2012, Pages 65-74

[3] S. Ghodrat, A.C. Riemslag, M. Janssen, J. Sietsma, L.A.I. Kestens, Measurement and characterization of Thermo-Mechanical Fatigue in Compacted Graphite Iron, International Journal of Fatigue, Volume 48, 2013, Pages 319-329

[4] M. Ekström, S. Jonsson, High-temperature mechanical- and fatigue properties of cast alloys intended for use in exhaust manifolds, Materials Science and Engineering: A,Volume 616, 2014,Pages 78-87

[5] A. Constantinescu, E. Charkaluk, G. Lederer, L. Verger, A computational approach to thermomechanical fatigue, International Journal of Fatigue, Volume 26, Issue 8, August 2004, Pages 805-818

[6] Garud,Y. A new approach to the evaluation of fatigue under multiaxial loadings (1981). Journal of Engineering Materials and Technology- Transactions of the ASME , 103(2):118?125.

[7] Skelton, R. P. "Energy criterion for high temperature low cycle fatigue failure." Materials science and technology 7.5 (1991): 427-440.

[8] Thalmair, S., Thiele, J., Fischersworring-Bunk, A., Ehart, R., Guillou, M., Cylinder heads for high power gasoline engines - Thermomechanical fatigue life prediction (2006) SAE Technical Papers, .

[9] Kharkhour, H., Morin, G. (2007). Thermal fatigue of exhaust manifolds: Contribution of numerical simulation to field reliability assessment. Bulletin-Cercle d'études des métaux, 17(17), 135.

[10] Gosar, A., Nagode, M., Energy dissipation under multiaxial thermomechanical fatigue loading (2013) International Journal of Fatigue, 48, pp. 223-230.

[11] Roger, F., Chidley, A., Thermo-mechanical fatigue design of automotive heat exchangers (2013) European Journal of Computational Mechanics, 22 (2-4), pp. 228-235.

[12] Szmytka, F., Salem, M., Rézaï-Aria, F., Oudin, A., Thermal fatigue analysis of automotive Diesel piston: Experimental procedure and numerical protocol (2015) International Journal of Fatigue, 73, pp. 48-57.

[13] Castro Güiza, G.M., Hormaza, W., Galvis E, A.R., Méndez Moreno, L.M., Bending overload and thermal fatigue fractures in a cast exhaust manifold (2017) Engineering Failure Analysis, 82, pp. 138-148.

[14] L. Rémy. Thermal mechanical fatigue (including thermal shock). In Editors in Chief: I. Milne, R. O. Ritchie, and B. Karihaloo, editors, Comprehensive Structural Integrity, pages 113-199. Pergamon, Oxford, 2003.

[15] S.K. Koh, Fatigue damage evaluation of a high pressure tube steel using cyclic strain energy density. International Journal of Pressure Vessels and Piping, 2002, vol. 79, no 12, p. 791-798.

[16] S. Amiable, S. Chapuliot, A. Constantinescu, A. Fissolo. A computational lifetime prediction of a thermal shock experiment. Part II: discussion on difference fatigue criteria. Fatigue & Fracture of Engineering Materials & Structures, 2006, 29(3), 219-227.

[17] S. Tabibian, E. Charkaluk, A. Constantinescu, F. Szmytka, A. Oudin. TMF criteria for Lost Foam Casting aluminum alloys. Fatigue & Fracture of Engineering Materials & Structures, 2013, vol. 36, no 4, p. 349-360.

[18] Korsunsky, A. M., Dini, D., Dunne, F. P., Walsh, M. J. (2007). Comparative assessment of dissipated energy and other fatigue criteria. International journal of fatigue, 29(9-11), 1990-1995.

[19] Tomkins, B. (1968). Fatigue crack propagation?an analysis. Philosophical magazine, 18(155), 1041-1066.

[20] Lamba, H. S. (1975). The J-integral applied to cyclic loading. Engineering Fracture Mechanics, 7(4), 693-703.

[21] S.Y. Zamrik, An investigation of strain cycling behavior of 7075-T6 aluminium under combined state of strain, NASA CR-72843. Washington, DC: National Aeronautics and Space Administration, 1972

[22] Taner Gocmez, Ali Awarke, Stefan Pischinger, A new low cycle fatigue criterion for isothermal and out-of-phase thermomechanical loading, International Journal of Fatigue, Volume 32, Issue 4, 2010, Pages 769-779,

[23] E. Charkaluk, A. Constantinescu, F. Szmytka, S; Tabibian. Probability density functions: From porosities to fatigue lifetime. International Journal of Fatigue, 2014, vol. 63, p. 127-136.

[24] H. Gao, A. Wang, E. Zio, G. Bai, An integrated reliability approach with improved importance sampling for low-cycle fatigue damage prediction of turbine disks, Reliability Engineering & System Safety, 2020,

[25] Szmytka, F., Oudin, A. (2013). A reliability analysis method in thermomechanical fatigue design. International Journal of Fatigue, 53, 82-91.

[26] Doudard, Cédric, and Sylvain Calloch. "Influence of hardening type on self-heating of metallic materials under cyclic loadings at low amplitude." European Journal of Mechanics-A/Solids 28.2 (2009): 233-240.

[27] V. Maurel, L. Rémy, F.Dahmen, N. Haddar. An engineering model for low cycle fatigue life based on a partition of energy and micro-crack growth. International Journal of Fatigue, 31(5), pages 952-961, 2009.

[28] Bavard, K., Bernhart, G., Zhang, X. P. (2003). High temperature low cycle fatigue of spheroidal graphite cast iron. International Journal of cast Metals research, 16(1-3), 233-238.

[29] Limodin, Nathalie, et al. "Application of X-ray microtomography to study the influence of the casting microstructure upon the tensile behaviour of an Al-Si alloy." Nuclear Instruments and Methods in Physics Research Section B: Beam Interactions with Materials and Atoms 324 (2014): 57-62.

[30] Murakami, Y., Endo, M. (1994). Effects of defects, inclusions and inhomogeneities on fatigue strength. International journal of fatigue, 16(3), 163-182

[31] Couper, M. J., Neeson, A. E., Griffiths, J. R. (1990). Casting defects and the fatigue behaviour of an aluminium casting alloy. Fatigue & Fracture of Engineering Materials & Structures, 13(3), 213-227.

[32] Skallerud, B., Iveland, T., Härkegård, G. (1993). Fatigue life assessment of aluminum alloys with casting defects. Engineering Fracture Mechanics, 44(6), 857-874.

[33] Dezecot, S., Brochu, M. (2015). Microstructural characterization and high cycle fatigue behavior of investment cast A357 aluminum alloy. International Journal of Fatigue, 77, 154-159.

[34] Viet-Duc Le, Franck Morel, Daniel Bellett, Nicolas Saintier, Pierre Osmond (2016), Multiaxial high cycle fatigue damage mechanisms associated with the different microstructural heterogeneities of cast aluminium alloys. Materials Science and Engineering: A, 649, 426-440

[35] Endo, M. (1989). Effects of graphite shape, size and distribution on the fatigue strength of spheroidal graphite cast irons. J. Soc. Mater. Sci., Jpn., 38(433), 1139-1144.

[36] Yaacoub Agha, H., Béranger, A. S., Billardon, R., Hild, F. (1998). High?cycle fatigue behaviour of spheroidal graphite cast iron. Fatigue & Fracture of Engineering Materials & Structures, 21(3), 287-296.

[37] Nadot, Y., Mendez, J., Ranganathan, N. A., Beranger, A. S. (1999). Fatigue life assessment of nodular cast iron containing casting defects. Fatigue & fracture of engineering materials & structures, 22(4), 289-300.

[38] Marrow, T. J., Buffiere, J. Y., Withers, P. J., Johnson, G., Engelberg, D. (2004). High resolution X-ray tomography of short fatigue crack nucleation in austempered ductile cast iron. International journal of fatigue, 26(7), 717-725.

[39] Nadot, Y., Mendez, J., Ranganathan, N. (2004). Influence of casting defects on the fatigue limit of nodular cast iron. International Journal of Fatigue, 26(3), 311-319.

[40] Costa, N., Machado, N., Silva, F. S. (2010). A new method for prediction of nodular cast iron fatigue limit. International Journal of Fatigue, 32(7), 988-995.

[41] Huetter, G., Zybell, L., Kuna, M. (2015). Micromechanisms of fracture in nodular cast iron: From experimental findings towards modeling strategies?A review. Engineering Fracture Mechanics, 144, 118-141.

[42] Lukhi, M., Kuna, M., Hütter, G. (2018). Numerical investigation of low cycle fatigue mechanism in nodular cast iron. International Journal of Fatigue, 113, 290-298.

[43] Mbiakop, A and Constantinescu, A and Danas, K, An analytical model for porous single crystals with ellipsoidal voids, Journal of the Mechanics and Physics of Solid, 84, 436-467, 2015=Pergamon

[44] M.J. Dong, C. Prioul, D. François. Damage effect on the fracture toughness of nodular cast iron: part I. Damage characterization and plastic flow stress modeling. Metallurgical and Materials Transactions A, 28(11), 2245-2254, 1997

[45] Seifert, T., Riedel, H. (2010). Mechanism-based thermomechanical fatigue life prediction of cast iron. Part I: Models. International Journal of Fatigue, 32(8), 1358-1367.

[46] F. Szmytka, L. Rémy, H. Maitournam, A. Köster, M.Bourgeois, New flow rules in elasto-viscoplastic constitutive models for spheroidal graphite cast-iron, International Journal of Plasticity, Volume 26, Issue 6, June 2010, Pages 905-924

[47] L. Rémy, F. Szmytka, L. Bucher, Constitutive models for bcc engineering iron alloys exposed to thermal-mechanical fatigue, International Journal of Fatigue, Volume 53, August 2013, Pages 2-14

[48] I. Hervas, M.B. Bettaieb, E. Hug. Damage mechanisms evolution of ductile cast irons under thermomechanical loadings. International Journal of Materials and Product Technology, 2013, vol. 47, no 1, p. 23-32.

[49] K. M. Pedersen, N. S. Tiedje, Graphite nodule count and size distribution in thin-walled ductile cast iron, Materials Characterization, Volume 59, Issue 8, August 2008, Pages 1111-1121, ISSN 1044-5803

[50] Takahashi, R., Sibuya, M. (2002). Metal fatigue, Wicksell transform and extreme values. Applied Stochastic Models in Business and Industry, 18(3), 301-312.

[51] Fullman, RL and others, Measurement of particle sizes in opaque bodie, 1953, General Electric Research Laboratory

[52] C. Verdu, J. Adrien, J.Y. Buffière, Three-dimensional shape of the early stages of fatigue cracks nucleated in nodular cast iron, Materials Science and Engineering: A, Volumes 483-484, 15 June 2008, Pages 402-405

[53] N. Bonora, A. Ruggiero, Micromechanical modeling of ductile cast iron incorporating damage. Part I: Ferritic ductile cast iron, International Journal of Solids and Structures, Volume 42, Issues 5-6, March 2005, Pages 1401-1424

[54] Harada S., Akiniwa Y., Ueda T., 1992. The effect of microstructure on the low-cycle fatigue behavior of ductile cast iron. In K.-T. Rie et al. (eds.), Low Cycle Fatigue and Elasto-Plastic Behaviour of Materials–3

[55] Komotori J., Shimizu M., 1998. Fracture mechanism of ferritic ductile cast iron in extremely low cycle fatigue. In: Rie K-T, Portella PD, editors. Low cycle fatigue and elastoplastic behaviour of materials. Netherlands: Springer, pp. 39–44

[56] Bubenko, L., Konecna, R., Nicoletto, G. (2009). Observation of fatigue crack paths in nodular cast iron and ADI microstructures. Materials Engineering, 16(3), 13.

[57] Canzar P., Tonkovic Z., Kodvanj J., 2012. Microstructure influence on fatigue behaviour of nodular cast iron. Materials Science and Engineering A556, 88–99

[58] Needleman, A., A Continuum Model for Void Nucleation by Inclusion Debonding., ASME. J. Appl. Mech. September 1987; 54(3): 525–531.

[59] Brocks, W., Hao, S., Steglich, D., 1996. Micromechanical modeling of the damage and toughnessbehavior of nodular cast iron materials. J. de Physique IV 6 C6, 43–52.

[60] Kuna, M., Sun, D.-Z., 1996. Analyses of void growth and coalescence in cast iron by cell models.J. de Physique IV 6 C6, 113–122.

[61] D. Steglich, W. Brocks, Micromechanical modelling of the behaviour of ductile materials including particles, Computational Materials Science, Volume 9, Issues 1–2, 1997, Pages 7-17,

[62] K.S. Zhang, J.B. Bai, D. François, Ductile fracture of materials with high void volume fraction, International Journal of Solids and Structures, Volume 36, Issue 23, 1999, Pages 3407-3425,

[63] C. Berdin, M.J. Dong, C. Prioul, Local approach of damage and fracture toughness for nodular cast iron, Engineering Fracture Mechanics, Volume 68, Issue 9, 2001, Pages 1107-1117,

[64] Lukhi M., Kuna M., Hütter G., 2018. Numerical investigation of low cycle fatigue mechanism in nodular cast iron. International Journal of Fatigue 113, 290–298

[65] Beretta, S. , Anderson, C and others, Extreme value statistics in metal fatigue, Riunione Scientifica della Società Italiana di Statistica, 251-260, 2002

[66] Dezecot, S., Maurel, V., Buffière, J. Y., Szmytka, F., Köster, A. (2017). 3D characterization and modeling of low cycle fatigue damage mechanisms at high temperature in a cast aluminum alloy. Acta Materialia, 123, 24-34.

[67] Mbiakop, A., Constantinescu, A. and Danas, K. , On void shape effects of periodic elasto-plastic materials subjected to cyclic loading, European Journal of Mechanics - A Solids, pages 481-499, 49, 2015

[68] F. Szmytka, L. Rémy, H.M. Maitournam, A. Köster, M. Bourgeois. New flow rules in elasto-viscoplastic constitutive models for spheroidal graphite cast-iron. International Journal of Plasticity, 26(6), 905-924, 2010

[69] Szmytka, F., Forré, A., Augustins, L. (2015). A time increment control for return mapping algorithm applied to cyclic viscoplastic constitutive models. Finite Elements in Analysis and Design, 102, 19-28.